ACS APPLIED MATERIALS & INTERFACES

Research Article

www.acsami.org

Antifouling, High-Flux Nanofiltration Membranes Enabled by Dual Functional Polydopamine

Yafei Li,[†] Yanlei Su,[†,‡] Xueting Zhao,[†] Xin He,[†] Runnan Zhang,[†] Jiaojiao Zhao,[†] Xiaochen Fan,[†] and Zhongyi Jiang*[,†,‡]

[†]Key Laboratory for Green Technology of Ministry of Education, School of Chemical Engineering and Technology, Tianjin University, Tianjin 300072, China

[‡]Collaborative Innovation Center of Chemical Science and Engineering (Tianjin), Tianjin 300072, China

ABSTRACT: A facile method for fabricating antifouling and high-flux nanofiltration (NF) membranes was developed based on bioinspired polydopamine (PDA). Polyethersulfone (PES) ultrafiltration membrane as the support was first deposited a thin PDA layer and then chemically modified by a new kind of fluorinated polyamine via Michael addition reaction between fluorinated polyamine and quinone groups of PDA. PDA coating significantly reduced the pore sizes of the PES support membrane and endowed the NF membrane with high separation performance (flux about 46.1 L/(m^2 h) under 0.1 MPa, molecular weight cutoff of about 780 Da). The grafted fluorinated polyamine on the PDA layer could form low free energy microdomains to impede the accumulation/coalescence of foulants and lower the adhesion force between foulants and the membrane, rendering the membrane surface with prominent fouling-release property. When foulant solutions (including bovine serum albumin, oil and humic acid) were filtered, the resultant NF membrane exhibited excellent antifouling properties (the minimal value of total flux decline ratio was ~8.9%, and the flux recovery ratio reached 98.6%). It is also found that the structural stability of the NF membrane could be significantly enhanced due to the covalent bond and other intermolecular interactions between the PDA layer and the PES support.

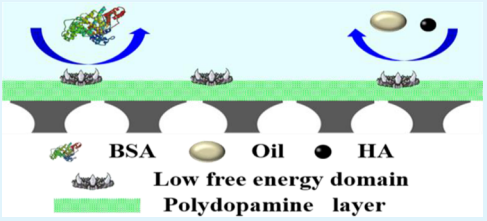

KEYWORDS: *polydopamine, nanofiltration membrane, low surface free energy, antifouling, high flux*

INTRODUCTION

Membrane-based water treatment technologies have attracted more interest in desalination and wastewater reclamation to increase the supply of water.[1,2] Nanofiltration (NF), a rapidly developing membrane separation technique, can effectively retain some salts, bacteria, viruses, pesticides and other organic contaminants from groundwater and wastewater streams.[3] Apart from drinking water treatment, NF produces very high quality permeate for irrigation or industrial applications such as cooling water.[4] In the new generation MBR-based treatment process, owing to its inherent advantages, NF has the potential to replace reverse osmosis (RO) for producing high quality water.[5] However, membrane fouling, due to settlement and accumulation of foulants (microorganisms, proteins and other organic molecules present in feed streams) on the membrane surface[6,7] would hinder wider applications of NF technology: on one hand, uncontrollable membrane fouling would lead to a loss of the membrane performance and thus increase the operating pressure requirement and chemical cleaning frequency to maintain the membrane performance; on the other hand, the short lifespan of membrane due to the damage of chemical cleaning would dramatically increase the maintenance cost of the membrane process.[8] Therefore, it is essential to construct antifouling membrane surfaces that decrease the adsorption/adhesion or increase the release of adsorbed foulants.

It is reported that membrane surface properties, such as hydrophilicity, roughness and charge would affect the fouling process.[9] To date, several methods have been developed to reduce membrane fouling, such as coating or grafting functional materials on the membrane,[9,10] incorporating nanostructured materials into the membranes[11,12] and fabricating new membranes with tailored chemistry.[13] Generally speaking, the majority of efforts are devoted to enhancing the fouling-resistant property of the membrane, that is to say, effectively preventing foulants from depositing at membrane surface. To the best of our knowledge, there is almost no public study about improving the fouling-release property of NF membranes.[14] Unlike fouling-resistant surfaces, the general idea of the fouling-release surface is to reduce the adhesion force between foulants and the surface for facilitating the removal of foulants by a simple hydraulic cleaning.[15] Increasing the fouling-release property should open a new door to tune the antifouling characteristics of NF membranes.

Low surface free energy materials have been reported to effectively enhance the fouling-release properties of the marine coating or ultrafiltration membrane. In the existing literatures, fouling-release coatings mainly include silicone-[16,17] and fluoropolymer-based binders,[18−21] which exhibit good fouling-

Received: December 26, 2013
Accepted: April 2, 2014
Published: April 2, 2014

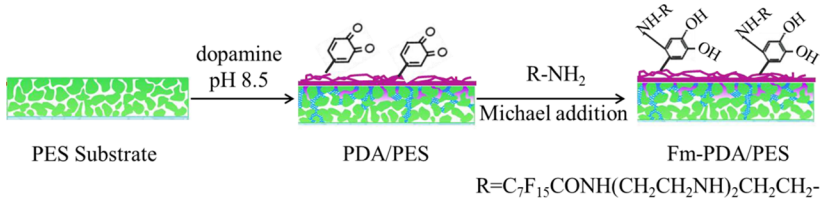

Figure 1. Schematic diagram of preparation and surface fluorination for the PDA/PES composite membrane.

release properties due to their low surface free energy nature.[22] The fouling-release surface utilized in the ultrafiltration membrane field has also attracted much attention. Zhu et al.[23] blend a synthesized fluorine-containing additive polymer (AP1) with polyvinylidene fluoride (PVDF) to obtain a novel ultrafiltration membrane with low surface free energy, which exhibited a good fouling-release property. In our previous research, a "forced surface segregation" method is first implemented to fabricate an ultrafiltration membrane with low surface free energy.[24] Fluorine-containing segments[24,25] and silicone segments,[26] as low surface free energy segments, are dragged onto membrane and pore surfaces by hydrophilic segments during the immersion–precipitation operation step, endowing the membrane with a superior fouling-release property. These studies clearly reveal the potential of using low surface free energy materials to combat surface fouling. No parallel research reports can be found for NF membranes. Due to the distinct differences of the membrane structure and preparation method between the NF membrane and ultrafiltration membrane, it is necessary to explore a facile and generic approach for engineering a NF membrane with an excellent fouling-release property.

Recently, polydopamine (PDA) coatings have drawn great interest as a versatile platform for application in membrane surface modification.[27−30] Besides the attractive adhesion property of PDA,[31] the quinone groups on PDA could react with thiol compounds[32] and nitrogen derivatives,[33,34] forming new membrane surfaces with desirable properties. In this study, the approach for preparing an antifouling NF membrane involved simple dip-coating of the PDA layer onto a PES ultrafiltration membrane (as the support), followed by conjugation of fluorinated polyamine to the PDA layer through Michael addition reaction. The PDA layer of the composite NF membrane exhibited two functions (i) reducing the pore sizes of PES support to reject dyes and (ii) providing reaction sites for further modification. The fluorinated polyamine grafted on the PDA layer was used to engineer a low free energy membrane surface for enhanced fouling-release property. The surface composition was analyzed by X-ray photoelectron spectroscopy (XPS) and Fourier transform infrared spectroscopy (FTIR). Scanning electron microscopy (SEM), atomic force microscopy (AFM) and contact angles were used to probe the morphology, roughness and hydrophilicity of the prepared membrane, respectively. The separation properties of the membranes were extensively tested by the filtration of dyes and the measurement of molecular weight cutoff (MWCO) using poly(ethylene glycol) (PEG). The structure stability and the antifouling properties of the prepared membrane were also investigated in detail.

EXPERIMENTAL SECTION

Materials. Polyethersulfone (PES) ultrafiltration membranes with MWCO 50 000 Da were supplied by the Development Center of Water Treatment Technology (Hangzhou, China). Dopamine hydrochloride was purchased from Yuancheng Technology Development Co. Ltd. (Wuhan, China). Tris(hydroxymethyl)aminomethane (Tris) was purchased from Sigma-Aldrich Chemical Co. The fluorinated polyamine ($C_7F_{15}COONH(CH_2CH_2NH)_2CH_2CH_2NH_2$) was synthesized by the condensation of perfluorooctanoic acid and triethylenetetramine as described in our previous study.[14] Hydrochloric acid (HCl) and humic acid (HA) were purchased from Kewei Chemical Reagent Co. (Tianjin, China). Dyes including Congo red, Orange GII and Methylene blue were also purchased from Kewei Chemical Reagent Co. (Tianjin, China). Bovine serum albumin (BSA) and high-speed vacuum pump oil (GS-1) as the two kinds of foulants were obtained from Institute of Hematology, Chinese Academy of Medical Science (Tianjin, China) and Beijing Sifang Special Oil Company (China), respectively. Sodium dodecyl sulfate (SDS) as the emulsifier in preparing the oil/water emulsion was purchased from Dingguo Changsheng Bio-Technology Co. (Beijing, China). All chemicals used in this study were not further purified. Water was deionized water at pH 6.0.

Preparation and Modification of the Composite Membrane. Dopamine solution (2.0 g/L) was prepared by dissolving 40 mg of dopamine hydrochloride in 20 mL Tris–HCl buffer solution (50 mM, pH 8.5). Circular pieces of PES ultrafiltration membrane (area of 28.7 cm^2) were submerged in the dopamine solution and shaken at 25 °C for a scheduled time (T). After that, the polydopamine coated membranes, named PDA/PES composite membrane, were taken out and rinsed in deionized water for 2 h (completely replaced with freshwater every 30 min) to remove most residual weakly bound polydopamine. The PDA/PES composite membrane was dried at 40 °C in a vacuum oven for 10 min and then further modified by grafting fluorinated polyamine with the method described in the literature.[27] Briefly, fluorinated polyamine was dissolved in a 10 mM Tris–HCl buffer solution (pH 8.5) and heated to 60 °C. The concentration of fluorinated polyamine ranged from 1.0 to 5.0 g/L. This solution was poured into a 100 mm diameter Petri plate and the PDA/PES composite membrane was floated, PDA-modified side down, on the fluorinated polyamine solution for a scheduled time in an oven at 60 °C. Then the fluorinated PDA/PES composite membrane was taken out and stored in deionized water before use. Figure 1 is the schematic diagram of the preparation and surface fluorination of the PDA/PES composite membranes. The fluorinated PDA/PES composite membranes were designated as Fm-PDA/PES, where the m indicates the fluorinated polyamine concentration of m g/L.

Characterization of the Composite Membrane. The surface morphology of the composite membrane was observed by SEM (Nanosem 430). The samples were gold-sputtered before SEM analysis. AFM (Nanoscope IIIA) was used to measure the roughness of the membranes and the measurement was performed in the tapping mode in air atmosphere. FTIR (Bruker Vertex 80 V) was used to investigate the chemical structure of the membranes. The spectra were collected at the spectral regions 400–4000 cm^{-1} with a resolution of 4 cm^{-1}. The experiments ran with air as the background and all the spectra were baseline corrected. An XPS (PHI-1600) instrument using Al Kα (1486.6 eV) as the radiation source was used to analyze the surface chemical composition of the membrane. The takeoff angle of photoelectron was set at 90° (the measured depth near 10 nm) and the survey spectra were 0–1100 eV. The static contact angle measurements of the membrane surfaces were conducted at 25 °C by a contact angle goniometer (JC2000C, Shanghai, China). Water, glycerol and diiodomethane were selected as test liquids to measure

the static contact angle. At least five measurements on each membrane were performed and the data were averaged to get a reliable value. Lifshitz–van der Waals acid–base model (three-liquid model) was used to calculate surface free energy (γ) of the membrane, which was expressed as follows:

$$\gamma_i = \gamma_i^{LW} + 2\sqrt{\gamma_i^+ \gamma_i^-} \quad (1)$$

$$\gamma_L(1 + \cos\theta) = 2\left(\sqrt{\gamma_s^{LW}\gamma_L^{LW}} + \sqrt{\gamma_s^+\gamma_L^-} + \sqrt{\gamma_s^-\gamma_L^+}\right) \quad (2)$$

In these equations, θ is the Young contact angle and i is denoted as either a solid (S) or a liquid (L) phase.γ_i^{LW}, γ_i^+ and γ_i^- (mJ/m^2) were the Lifshitz–van der Waals and acid and base components, respectively.

Separation Performance of the Composite Membrane. The separation performance tests of the PDA/PES composite membrane and the fluorinated PDA/PES composite membrane were conducted at 0.10 MPa and a temperature of 25 ± 1 °C with a dead-end stirred-cell filtration system. The system consisted of a filtration cell (effective area 28.7 cm^2, model 8200, Millipore Co.), a solution reservoir (with volume of 1.0 L) and a nitrogen gas cylinder. The operation pressure was maintained by nitrogen gas in the system. Deionized water and deionized water containing 100 mg/L dyes (including Orange GII, Congo red, and Methylene blue) were utilized as the feed for testing the pure water flux and dye retention performance. Deionized water with poly(ethylene glycol) (PEG) of different molecular weights (200, 400, 600, 1000 and 2000 Da) were chosen as model solutes in the filtration experiments to test the MWCO of the fluorinated PDA/PES composite membrane. The feed pH in the tests was about 6.0 ± 0.2.

All the membrane samples were pressurized at 0.15 MPa with deionized water for stable membrane before test. After that, the pressure was lowered down to 0.10 MPa and water flux J_{w1} (L/(m^2 h)) was calculated according to eq 3:

$$J_{w1} = \frac{V}{A\Delta t} \quad (3)$$

where V, A and Δt represent the volume of permeated water, the membrane area and the permeation time, respectively. The retention performances were measured with dye aqueous solutions or deionized water with PEGs and the observed solute rejection rate (R) was calculated from the following equation:

$$R = \left(1 - \frac{C_p}{C_f}\right) \times 100\% \quad (4)$$

where C_p and C_f are the solute concentrations in permeate and feed, respectively. Dye concentrations were determined by measuring absorbance of dye with a UV–Vis spectrophotometer (UV-2800, Hitachi Co., Japan). The wavelength was set at the maximal absorption wavelength of Orange GII, Congo red, and Methylene blue (485, 490 and 660 nm, respectively) in filtration of the corresponding solution. PEG concentrations were determined by measuring absorbance at 535 nm after iodine complexation with a UV–Vis spectrophotometer.[35] All results presented are average data from three samples of each membrane type.

The structural stability of the fluorinated PDA/PES composite membrane (F3-PDA/PES) was examined by alcohol treatment. F3-PDA/PES membrane was immersed in absolute alcohol for 24, 48, 72, 96, 120 and 144 h to let the PES support fully swell. Then, the swollen F3-PDA/PES membrane was taken out and fully washed with deionized water to remove remaining alcohol. The water flux and rejection of Orange GII were measured before and after alcohol treatment through the aforementioned methods, and the stability of F3-PDA/PES membrane was evaluated according to the extent of performance deterioration after alcohol treatment.

Antifouling Properties of the Composite Membrane. To characterize the antifouling properties (including fouling-resistant and fouling-release properties) of the PDA/PES and the F3-PDA/PES membrane, three kinds of model foulant solutions were used in the listed order: oil/water emulsion (GS-1, 1000 ppm; SDS as emulsifier, 100 ppm), HA aqueous solution and BSA aqueous solution (1000 ppm; dissolving 1 g HA or BSA in 1L deionized water). The long-time antifouling experiment mainly included three steps: the pure water flux J_{w1} (L/(m^2 h)) was first measured at a transmembrane pressure of 0.1 MPa for 2 h. Then, the solution reservoir and filtration cell were emptied and refilled rapidly with deionized water and foulant solution, respectively. The flux for foulant solution J_p (L/(m^2 h)) was measured under 0.1 MPa for 24 h. In the third step, the fouled membranes were washed for 30 min with deionized water, and the pure water flux of cleaned membranes J_{w2} (L/(m^2 h)) was measured.

Several indexes, including the flux recovery ratio (FRR), total flux decline ratio (DR_t), reversible flux decline ratio (DR_r) and irreversible flux decline ratio (DR_{ir}), were used to evaluate the antifouling property of the membrane. They were defined as follows:

$$FRR = \left(\frac{J_{w2}}{J_{w1}}\right) \times 100\% \quad (5)$$

$$DR_t = \left(\frac{J_{w1} - J_p}{J_{w1}}\right) \times 100\% \quad (6)$$

$$DR_r = \left(\frac{J_{w2} - J_p}{J_{w1}}\right) \times 100\% \quad (7)$$

$$DR_{ir} = \left(\frac{J_{w1} - J_{w2}}{J_{w1}}\right) \times 100\% \quad (8)$$

The lower DR_t and higher FRR values of the membranes represented a better antifouling property. The lower DR_{ir} denoted that the foulants were easily swept away from the membrane surface by water washing.

RESULTS AND DISCUSSION

Surface Morphologies of the Composite Membranes. Dopamine could polymerize to form thin adherent PDA coatings on any surface, including organic and inorganic surfaces.[33] According to the published literature,[27,36] dopamine was easily oxidized by the dissolved oxygen of solution at alkaline pHs, generating 5,6-dihydroxyindole (DHI) via intramolecular oxidation. Then DHI underwent oxidative polymerization and noncovalent self-assembly to produce PDA particles and aggregates, which were then deposited on the substrate surface, forming a continuous PDA film on the substrate.[37] The surface morphologies of the PES support, PDA/PES, F3-PDA/PES and F5-PDA/PES membranes are shown in Figure 2. Figure 2a shows the relatively smooth surface of the PES support and some pores, whose diameter were about 10–20 nm, were observed (Figure 2a′). However, the pores were almost invisible (Figure 2b′) and some particles appeared on the PDA/PES membrane surface (Figure 2b). These results were attributed to the deposited PDA particles on the pore walls as well as on the surface of the PES support, forming a PDA coating on the support and drastically reducing the pore sizes. Jiang et al.[37] and Wei et al.[38] also observed the analogous nanoparticles in their previous reports. The particles and aggregates were incorporated into the PDA film by covalent bonding, π stacking and other noncovalent interactions.[38] Figure 2c,d shows the images for F3-PDA/PES and F5-PDA/PES membrane, respectively. Figure 2c′,d′ shows the high resolution images for F3-PDA/PES and F5-PDA/PES membranes, respectively. Compared with PDA/PES composite membrane, the surface was much smoother after grafting fluorinated polyamine.

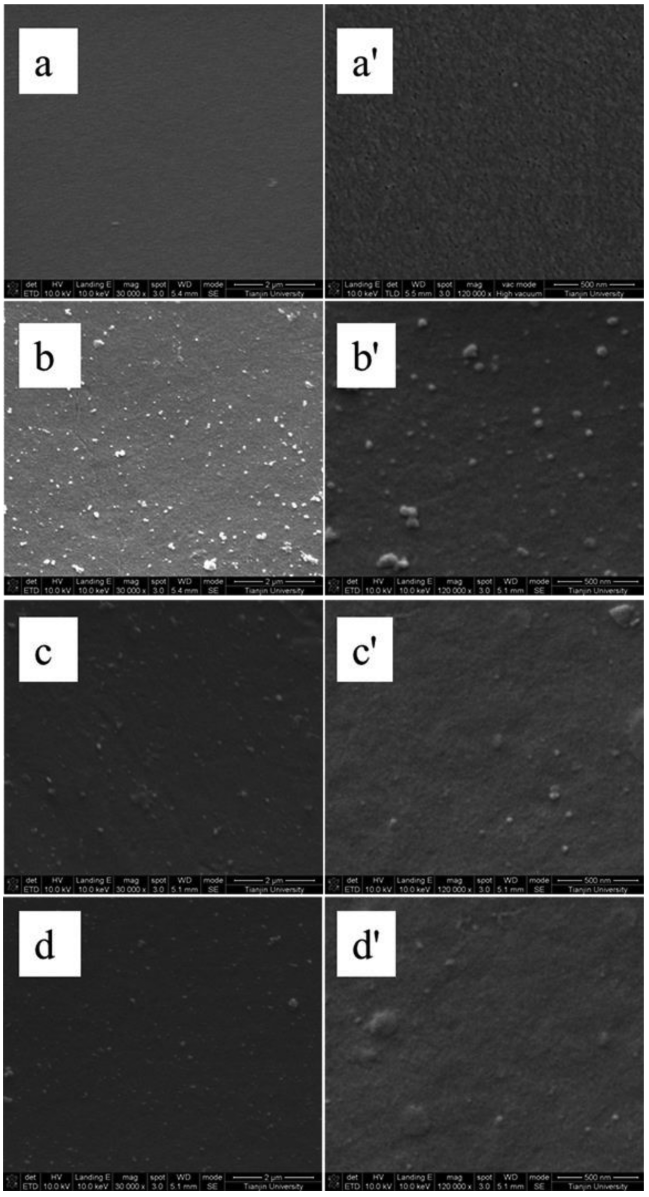

Figure 2. Surface SEM morphology of (a) PES, (b) PDA/PES, (c) F3-PDA/PES and (d) F5-PDA/PES membranes. Panels a′, b′, c′ and d′ are the high resolution images of surface for PES, PDA/PES, F3-PDA/PES and F5-PDA/PES, respectively.

AFM was used to examine the surface roughness of the membrane in this study. The 4 × 4 μm three-dimensional AFM images and the average roughness of PES support, the composite membranes with and without modification are shown in Figure 3. The mean roughness (Ra) increased from 3.4 ± 0.3 nm of PES support to 8.1 ± 0.8 nm of PDA/PES composite membrane due to the deposited PDA nanoparticles on the membrane surface. The mean roughness (Ra) decreased from 8.1 ± 0.8 nm (PDA/PES) to 6.7 ± 0.6 nm (F3-PDA/PES) and 5.0 ± 0.6 nm (F5-PDA/PES) after grafting fluorinated polyamine onto the PDA/PES composite membrane, which was possibly attributed to the presence of fluorinated polyamine within the concavities of the PDA/PES membrane surface. These results were consistent with qualitative SEM observations.

Chemical Structures and Compositions of the Composite Membranes. Figure 4 exhibits the FTIR spectra of the PES support, PDA/PES, F1-PDA/PES, F3-PDA/PES and F5-PDA/PES membranes. As observed from FTIR spectra of Figure 4, the PDA/PES membrane showed very similar FTIR spectra compared with the PES support, except the two distinct bands at about 1516 and 1660 cm^{-1}. The peaks at 1516 and 1660 cm^{-1} were in correspondence to the N—H deformation vibration and C═C stretching vibration in polydopamine, respectively, indicating the PDA layer had been successfully fixed onto the PES membrane. Compared with the PDA/PES composite membrane, the FTIR spectra of the fluorinated composite membranes (F1-PDA/PES, F3-PDA/PES, F5-PDA/PES) showed another new peak at 1361 cm^{-1}. This peak was corresponding to the C—F stretching bands, confirming the fluorinated polyamine had been immobilized on the PDA/PES composite membrane surface.

Furthermore, XPS analysis was used to determine surface compositions of the membranes. The XPS spectra of PES support, PDA/PES, F3-PDA/PES and F5-PDA/PES membranes are presented in Figure 5 and the XPS data of element contents on the membrane surface are given in Table 1. Compared with PES support, the new nitrogen element appeared on the spectrum of the PDA/PES composite membrane, which was attributed to the PDA layer containing amino groups (the source of nitrogen element). The F 1s peak at 687.0 eV appeared on the fluorinated composite membrane (F3-PDA/PES, F5-PDA/PES) demonstrated that the fluorinated polyamine was successfully grafted onto the PDA layer. Figure 5b presents a high-resolution XPS spectrum of C 1s and curve fitting of the F3-PDA/PES membrane. The C 1s of the F3-PDA/PES membrane could be resolved into five peaks at binding energies of 284.6, 285.7, 287.3, 291 and 293.2 eV, which were attributed to C—C, C—N (C—O), C═O, CF_2 and CF_3, respectively. The fluorinated polyamine was the only source of CF_2 and CF_3, which further indicated that the fluorinated polyamine had been successfully grafted onto the PDA layer. Table 1 shows that the atom percentage of sulfur declined from 2.5% of PES support to 1.1% of PDA/PES composite membrane and the atom percentage of nitrogen was 4.0% on surface of PDA/PES composite membrane, confirming the PDA layer was covered on PDA/PES composite membrane. The appearance of sulfur on PDA/PES composite membrane could be interpreted that the thickness of the PDA layer was less than the detection depth of XPS measurements (~10 nm) in this study. The thickness of the PDA layer agreed well with that reported by Zangmeister et al.[39] The atom percentage of fluorine rose from 26.5% of F3-PDA/PES to 27.4% of F5-PDA/PES, suggesting that the amount of grafted fluorinated polyamine increased slightly after the concentration of fluorinated polyamine reached 3.0 g/L.

The surface hydrophilicity of the PDA/PES composite membrane and all the fluorinated PDA/PES composite membranes were confirmed by static water contact angle measurements, as shown in Table 2. The PDA/PES composite membrane had a low contact angle of 43.5°, corresponding to high hydrophilicity. After fluorinated polyamine was grafted onto the PDA/PES composite membrane surface, the contact angles were remarkably increased from 43.5° to 87.0° for the F5-PDA/PES membrane. The high contact angle value of the F5-PDA/PES membrane was due to the hydrophobic nature of grafted perfluoroalkyl groups. The surface free energy (γ) calculated using the three-liquid model, as well as dispersive (γ^D) and polar components (γ^P) expressed by Owens and Wendt,[40] are also given in Table 2. Table 2 summarizes the

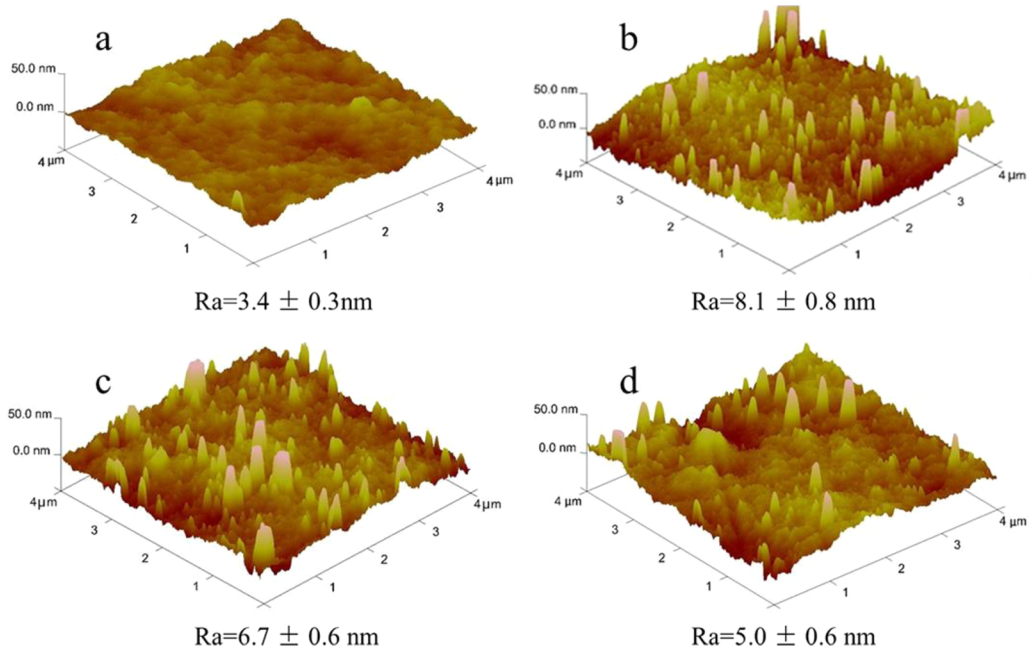

Figure 3. AFM morphology of (a) PES, (b) PDA/PES, (c) F3-PDA/PES and (d) F5-PDA/PES membranes.

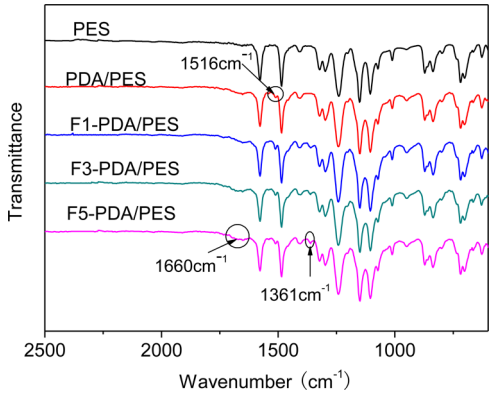

Figure 4. FTIR spectra of PES, PDA/PES, F1-PDA/PES, F3-PDA/PES and F5-PDA/PES membranes.

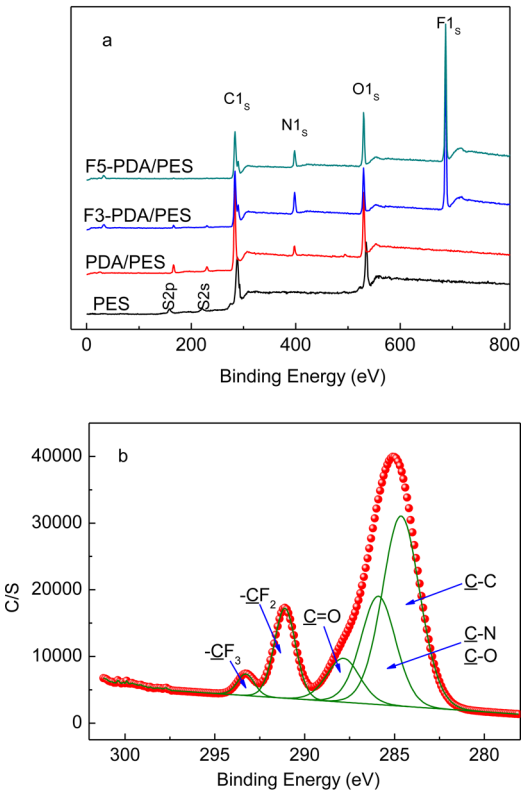

Figure 5. (a) XPS spectrum of PES, PDA/PES and F3-PDA/PES membrane and (b) high-resolution XPS spectrum of C 1s region of F3- PDA/PES membrane.

obvious decrease of γ, along with γ^D and γ^P, for the fluorinated PDA/PES composite membrane compared with the PDA/PES composite membrane. For example, the surface free energy (γ) decreased from 56.5 mJ/m^2 for the PDA/PES composite membrane to 27.4 mJ/m^2 for the F5-PDA/PES membrane. The values of surface free energy lay in the low adhesion zone according to the "Baier curve".[41] Hence, the low surface free energy property would endow the fluorinated PDA/PES composite membranes with good fouling-release properties due to the minimal adhesion propensity and reduced opportunities for the interfacial molecular interactions between foulants and membrane surface.[15,42,43]

Separation Performance of the Composite Membranes. Because the preparation conditions greatly influenced the permeability of the composite membranes, a series of experiments was implemented to optimize the conditions for the preparation of the thin active layer, such as dopamine polymerization time, grafting reaction time and fluorinated amine concentration. The effect of dopamine polymerization time on the performance of PDA/PES composite membrane was first studied. As shown in Figure 6, water flux was dramatically decreased from 81.6 to 15.1 L/(m^2 h) and the Orange GII rejection was increased from 38.5% to 76.7% with increasing dopamine polymerization time from 15 to 180 min. It is proposed that the dopamine polymerization time exerted a pronounced influence on the structure of the PDA layer. From the perspective of the PDA formation mechanism, the quinone groups of oxidized dopamine and the primary amino groups of

dx.doi.org/10.1021/am405990g | ACS Appl. Mater. Interfaces 2014, 6, 5548−5557

Table 1. Surface Elemental Composition of PES, PDA/PES, F3-PDA/PES and F5-PDA/PES Membranes

	surface elemental composition (mol %)				
membrane	C	O	S	N	F
PES	70.4	27.1	2.5		
PDA/PES	68.9	25.5	1.1	4.5	
F3-PDA/PES	52.3	13.2	0.6	7.4	26.5
F5-PDA/PES	50.9	12.8	0.1	8.8	27.4

Table 2. Water Contact Angles and Surface Free Energy Parameters of the Pristine Composite Membrane and the Fluorinated Composite Membrane

		surface free energy (mJ/m^2)		
membrane	water contact angle (deg)[a]	γ	γ^D	γ^P
PDA/PES	43.5	56.5	45.2	11.3
F1-PDA/PES	80.3	31.0	21.5	9.5
F2-PDA/PES	82.1	30.3	19.6	10.7
F3-PDA/PES	83.5	28.2	17.0	11.2
F4-PDA/PES	85.3	28.1	15.6	12.5
F5-PDA/PES	87.0	27.4	15.0	12.4

[a]The error in contact angle measurement was no more than 2°.

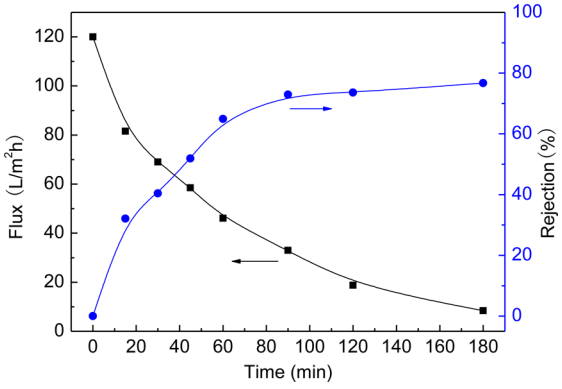

Figure 6. Effect of dopamine polymerization time on the performance of PDA/PES composite membrane (experiments performed at 0.1 MPa, using 100 mg/L Orange GII solution as feed).

dopamine could form PDA network through Schiff base formation and/or by Michael type addition.[44] Increasing polymerization time resulted in a thicker and more compact PDA layer, which dominated the separation performance of composite membrane. According to the results shown above, the polymerization time was fixed at 60 min in the following experiments. The membrane prepared in this condition possessed a flux of 46.1 L/(m^2 h) under 0.1 MPa and Orange GII rejection ratio of 64.9%.

After polymerization for 60 min, the PDA/PES composite membrane was submerged in the fluorinated polyamine aqueous solution with content of 5.0 g/L at 60 °C for a scheduled time varying from 0.5, 1, 2, 3 to 4 h. The influence of grafting time on the performance of the composite membranes is given in Figure 7. The decrease of the water flux from 46.1 to 40.0 L/(m^2 h) showed that grafted fluorinated polyamine on the composite membrane would hinder the pass of water due to the increase of membrane resistance. The little variation of Orange GII rejection suggested that the grafted fluorinated polyamine did not greatly impair rejection performance of the

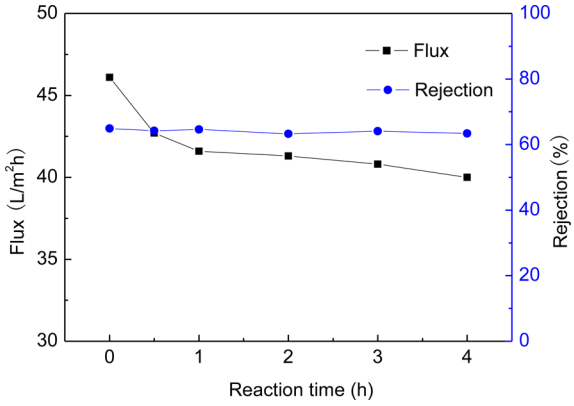

Figure 7. Effect of grafting reaction time on the performance of modified PDA/PES composite membrane (experiments performed at 0.1 MPa, using 100 mg/L Orange GII solution as feed).

membrane with increasing the grafting time. The reason is presumably that the structure of PDA layer was not significantly changed by grafting fluorinated polyamine onto the PDA/PES membrane. Hence, the grafting time was fixed at 1 h in the following study.

Effect of fluorinated amine concentration on the separation performance of composite membranes was studied and is presented in Figure 8. The permeate flux of the composite

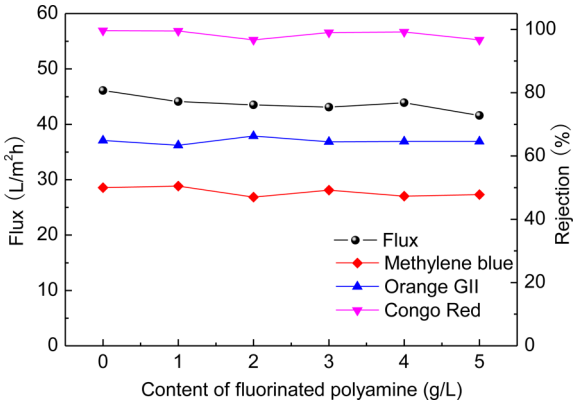

Figure 8. Effect of fluorinated polyamine concentration on the performance of modified PDA/PES composite membrane.

membrane was decreased from 46.1 L/(m^2 h) of PDA/PES to 44.1, 43.5, 43.1, 43.9 and 41.6 L/(m^2 h) with an increase of fluorinated amine concentration from 0 to 1.0, 2.0, 3.0, 4.0 and 5.0 g/L. The decrease of flux could be attributed to the increase of membrane mass-transfer resistance after grafting fluorinated polyamine. However, the rejections of the composite membrane to Methylene blue, Orange GII and Congo red only exhibited slight fluctuations with the increase of the fluorinated polyamine solution concentration, which further affirmed that the surface grafting did not affect the rejection of composite membrane in this study. The mean rejections of the studied composite membrane to different dyes followed the order of Congo red (99%, M_W: 696) > Orange GII (64%, M_W: 452) > Methylene blue (50%, M_W: 320).

The separation performance of a membrane can be also expressed by its molecular weight cutoff. In this study, the MWCO value of the F3-PDA/PES membrane was taken by molecular weight of PEGs that were rejected by this membrane to 90%. Figure 9 illustrated the observed rejection ratio of the

dx.doi.org/10.1021/am405990g | ACS Appl. Mater. Interfaces 2014, 6, 5548−5557

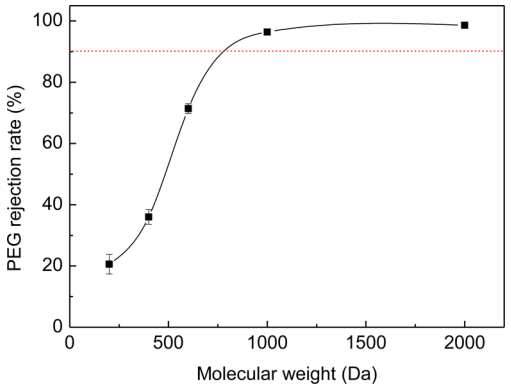

Figure 9. PEG rejection as a function of molecular weight for the F3-PDA/PES membrane tested with 50 mg/L PEG aqueous solution at 0.1 MPa and 25.0 °C.

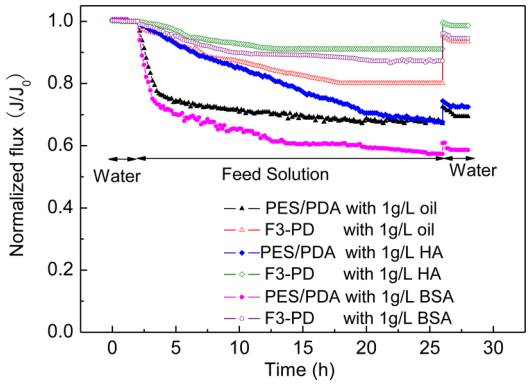

Figure 10. Time-dependent normalized flux for PDA/PES and F3-PDA/PES membranes during the filtration of BSA, HA and oil solution. The nanofiltration process included four steps: pure water filtration, foulant filtration of fresh membranes, water cleaning of membranes (not shown), and pure water filtration of pure water cleaning membranes. Nanofiltration was carried out at a temperature of 25 °C and the operation pressure was 0.1 MPa.

studied membrane (F3-PDA/PES) to the five different PEGs (200, 400, 600, 1000 and 2000 Da) under 0.1 MPa. The MWCO of the F3-PDA/PES membrane was around 780 Da, which was in the range of nanofiltration. It should be noted that the flux of resultant membranes ranged between 40 and 46 L/(m^2 h) under 0.1 MPa, roughly 2−4 times higher than that of the nanofiltration membranes with similar MWCO.[45−48] The composite membranes with high fluxes have potential applications in texile wastewater treatment and other fields.

Antifouling Properties of the Composite Membranes. During the membrane filtration process, the reversible foulant deposition or concentration polarization and the adsorption or direct attachment of foulants on membrane surface could lead to severe membrane fouling and drastic flux decline. Three foulants were selected (BSA as a representative protein, HA representing natural organic matter and oil as a representative hydrocarbon) to examine the antifouling properties of the PDA/PES composite membrane and the fluorinated PDA/PES composite membrane. Because the foulants involved in this study (larger than the pores of the composite membrane) could not penetrate into the membrane pores, they would only cause surface fouling.

The time-dependent normalized flux variations of PDA/PES and F3-PDA/PES membranes during BSA solution filtration are presented in Figure 10. In the initial operation, the buildup of the concentration polarization layer caused by consolidation and aggregation of solute and severe membrane fouling caused by deposition and adsorption of BSA led to a drastic flux decline. In the subsequent operation, a stable flux was obtained due to the equilibrium of deposition and resuspension of the solute, which was attributed to the rigorous stirring near the membrane surface. Finally, the flux of cleaned membrane (washed with deionized water) was recovered to a certain extent. As shown in Table 3, the DR_t value of the PDA/PES composite membrane was 42.6% (DR_r about 1.2%, DR_{ir} about 41.4%) and the FRR value of the PDA/PES composite membrane was 58.6%. The marked irreversible flux decline indicated serious membrane fouling took place during BSA filtration process and that the adsorbed BSA was difficult to remove from the membrane surface by simple hydraulic cleaning. Compared with PDA/PES composite membrane, the F3-PDA/PES membrane showed larger FRR, which was 94.5%. The DR_t, DR_{ir} and DR_r values decreased to 12.7%, 7.2% and 5.5%, respectively. The enhanced antifouling performance, especially the fouling-release property of fluorinated PDA/PES membrane was closely related to the low surface free energy of the membrane, which could effectively combat biofouling on the membrane surface.[49]

Table 3. Antifouling Indexes (DR_t, DR_r, DR_{ir} and FRR) of the composite membrane during BSA, HA solution and oil/water emulsion filtration measurements

	BSA		HA		oil	
antifouling indexes (%)	PDA/PES	F3-PDA/PES	PDA/PES	F3-PDA/PES	PDA/PES	F3-PDA/PES
FRR	58.6	94.5	72.4	98.6	69.4	93.4
DR_t	42.6	12.7	32.4	8.9	32.2	20.0
DR_r	1.2	7.2	4.8	7.5	1.6	13.4
DR_{ir}	41.4	5.5	27.6	1.4	30.6	6.6

During filtration of the oil/water emulsion, severe flux decline and poor flux recovery of PDA/PES membrane were observed. The corresponding DR_t was as high as about 32.2% (DR_r about 1.6%, DR_{ir} about 30.6%) and FRR value was 69.4%. After fluorination treatment, the F3-PDA/PES membrane exhibited reduced level of fouling (DR_t 20.0%) and increased flux recovery (FRR about 93.4%). The DR_{ir} value was only 6.6%, indicating that simple hydraulic cleaning could easily remove most of the adsorbed and deposited oil droplets on the membrane surface. We could conclude that the oil release property was considerably improved after grafting fluorinated polyamine onto the PDA/PES composite membrane surface. The remarkable alleviation of irreversible flux decline could be ascribed to the low surface free energy microdomains (forming by fluorinated polyamine) on the fluorinated PDA/PES composite membrane and the moderate shear force. The former prevented the coalescence/migration of oil droplets and the latter could sweep oil droplets away from the membrane surface.[43]

Figure 10 shows that the PDA/PES composite membrane underwent serious fouling and poor flux recovery during filtration of the HA solution. The corresponding DR_t reached to a high level, about 32.4% (DR_r about 4.8%, DR_{ir} about 27.6%) and FRR value was 72.4%. After fluorination treatment, the F3-PDA/PES membrane exhibited only 8.9% total flux decline and the irreversible flux decline ratio was merely 1.4%

dx.doi.org/10.1021/am405990g | ACS Appl. Mater. Interfaces 2014, 6, 5548−5557

in the 24 h filtration of HA solution. The F3-PDA/PES membrane maintained about 98.6% permeation flux after 30 min water washing. The fairly improved antifouling property could be also attributed to the low surface free energy microdomains of the F3-PDA/PES membrane, which facilitated the release of adsorbed or deposited HA molecular on the membrane surface. In this study, foulants (BSA, oil, HA) were much easier to be evicted away from the Fm-PDA/PES membranes surface, thus endowing those membranes with improved antifouling performance.

Structural Stability of the Composite Membranes. According to the previous report,[50] alcohol could swell the PES support but not seriously destroy its structure. The swelling of the support would cause the active layer of composite membranes to be detached from the support and, consequently, damage the separation performance.[51] To examine the structural stability of prepared composite membrane, the F3-PDA/PES membrane without/with alcohol treatment for various periods was tested with a 0.1 g/L Orange GII aqueous feed.

As shown in Figure 11, water flux and Orange GII rejection of the F3-PDA/PES membrane had a little variation after alcohol treatment for 144 h. The F3-PDA/PES membrane preserved the separation performance: water flux under 0.1 MPa was 43.4 L/(m^2 h) and rejection of Orange GII was 64%. The result evidently suggested that the F3-PDA/PES membrane had a good durability under alcohol treatment. It was speculated that the good structural stability of the resultant composite membrane was closely related to the strong adhesion between PDA and the PES support, achieved via covalent bond and other strong intermolecular interactions.[52] Robust and multiple interfacial binding forces between the support and the active layer (PDA layer) would enhance the interfacial compatibility and raise the structural stability of the composite membrane.

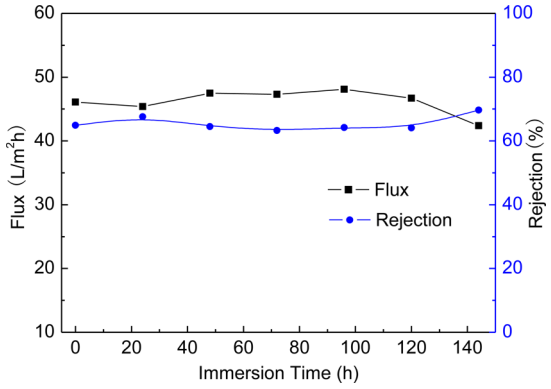

Figure 11. Effect of alcohol treatment on the performance of F3-PDA/PES membrane (experiments performed at 0.1 MPa, using 100 mg/L Orange GII solution as feed).

CONCLUSIONS

A facile method for fabricating antifouling and high-flux nanofiltration membranes was developed enabled by polydopamine (PDA). Polyethersulfone (PES) ultrafiltration membrane as the support was first deposited a thin PDA layer and then chemically modified by fluorinated polyamine via Michael addition reaction to prepare a composite NF membrane. PDA played the following two important roles: (1) reduced the pore sizes of PES support membrane, rendering membranes improved pore structure and (2) provided the active cites for fluorinated polyamine grafting to form low free energy microdomains onto membrane surface, rendering membranes improved surface structure. When using BSA, HA and oil as three model foulants, the composite NF membrane exhibited excellent antifouling properties, particularly the fouling-release property. During filtration of dye solution, the membranes acquired rejection of Congo red above 99% with a flux about 46 L/(m^2 h) under 0.1 MPa. After alcohol treatment for 144 h, the composite NF membrane exhibited good structural stability due to the strong and multiple interactions between the PDA layer and PES support.

AUTHOR INFORMATION

Corresponding Author

*Z. Jiang. E-mail: zhyjiang@tju.edu.cn. Fax: 86-22-27406646. Tel: 86-22-27406646.

Notes

The authors declare no competing financial interest.

ACKNOWLEDGMENTS

This research is financially supported by National Science Fund for Distinguished Young Scholars (21125627), Tianjin Natural Science Foundation (No. 13JCYBJC20500) and the Program of Introducing Talents of Discipline to Universities (No. B06006).

REFERENCES

(1) Elimelech, M.; Phillip, W. A. The Future of Seawater Desalination: Energy, Technology, and the Environment. *Science* **2011**, *333*, 712−717.

(2) Tiraferri, A.; Kang, Y.; Giannelis, E. P.; Elimelech, M. Highly Hydrophilic Thin-Film Composite Forward Osmosis Membranes Functionalized with Surface-Tailored Nanoparticles. *ACS Appl. Mater. Interfaces* **2012**, *4*, 5044−5053.

(3) Tang, Z.; Qiu, C.; McCutcheon, J. R.; Yoon, K.; Ma, H.; Fang, D.; Lee, E.; Kopp, C.; Hsiao, B. S.; Chu, B. Design and Fabrication of Electrospun Polyethersulfone Nanofibrous Scaffold for High-Flux Nanofiltration Membranes. *J. Polym. Sci., Part B: Polym. Phys.* **2009**, *47*, 2288−2300.

(4) Kappel, C.; Kemperman, A.; Temmink, H.; Zwijnenburg, A.; Rijnaarts, H.; Nijmeijer, K. Impacts of NF Concentrate Recirculation on Membrane Performance in an Integrated MBR and NF Membrane Process for Wastewater Treatment. *J. Membr. Sci.* **2014**, *453*, 359−368.

(5) Shannon, M. A.; Bohn, P. W.; Elimelech, M.; Georgiadis, J. G.; Marinas, B. J.; Mayes, A. M. Science and Technology for Water Purification in the Coming Decades. *Nature* **2008**, *452*, 301−310.

(6) Rana, D.; Matsuura, T. Surface Modifications for Antifouling Membranes. *Chem. Rev.* **2010**, *110*, 2448.

(7) Geise, G. M.; Lee, H. S.; Miller, D. J.; Freeman, B. D.; McGrath, J. E.; Paul, D. R. Water Purification by Membranes: The Role of Polymer Science. *J. Polym. Sci., Part B: Polym. Phys.* **2010**, *48*, 1685−1718.

(8) Vatanpour, V.; Madaeni, S. S.; Moradian, R.; Zinadini, S.; Astinchap, B. Novel Antibifouling Nanofiltration Polyethersulfone Membrane Fabricated from Embedding TiO_2 Coated Multiwalled Carbon Nanotubes. *Sep. Purif. Technol.* **2012**, *90*, 69−82.

(9) Van Wagner, E. M.; Sagle, A. C.; Sharma, M. M.; La, Y.-H.; Freeman, B. D. Surface Modification of Commercial Polyamide Desalination Membranes Using Poly(ethylene glycol) Diglycidyl Ether to Enhance Membrane Fouling Resistance. *J. Membr. Sci.* **2011**, *367*, 273−287.

(10) Tiraferri, A.; Vecitis, C. D.; Elimelech, M. Covalent Binding of Single-Walled Carbon Nanotubes to Polyamide Membranes for

Antimicrobial Surface Properties. *ACS Appl. Mater. Interfaces* **2011**, *3*, 2869−2877.
(11) Singh, A. K.; Singh, P.; Mishra, S.; Shahi, V. K. Anti-Biofouling Organic-Inorganic Hybrid Membrane for Water Treatment. *J. Mater. Chem.* **2012**, *22*, 1834−1844.
(12) Lee, H. S.; Im, S. J.; Kim, J. H.; Kim, H. J.; Kim, J. P.; Min, B. R. Polyamide Thin-Film Nanofiltration Membranes Containing TiO_2 Nanoparticles. *Desalination* **2008**, *219*, 48−56.
(13) Mo, Y.; Tiraferri, A.; Yip, N. Y.; Adout, A.; Huang, X.; Elimelech, M. Improved Antifouling Properties of Polyamide Nanofiltration Membranes by Reducing the Density of Surface Carboxyl Groups. *Environ. Sci. Technol.* **2012**, *46*, 13253−13261.
(14) Li, Y.; Su, Y.; Zhao, X.; Zhang, R.; Zhao, J.; Fan, X.; Jiang, Z. Surface Fluorination of Polyamide Nanofiltration Membrane for Enhanced Antifouling Property. *J. Membr. Sci.* **2014**, *455*, 15−23.
(15) Callow, J. A.; Callow, M. E. Trends in the Development of Environmentally Friendly Fouling-Resistant Marine Coatings. *Nat. Commun.* **2011**, *2*, 244.
(16) Sundaram, H. S.; Cho, Y.; Dimitriou, M. D.; Weinman, C. J.; Finlay, J. A.; Cone, G.; Callow, M. E.; Callow, J. A.; Kramer, E. J.; Ober, C. K. Triblock Copolymers with Grafted Fluorine-Free, Amphiphilic, Non-Ionic Side Chains for Antifouling and Fouling-Release Applications. *Biofouling* **2011**, *27*, 589−602.
(17) Cho, Y.; Sundaram, H. S.; Weinman, C. J.; Paik, M. Y.; Dimitriou, M. D.; Finlay, J. A.; Callow, M. E.; Callow, J. A.; Kramer, E. J.; Ober, C. K. Fluorine-Free Mixed Amphiphilic Polymers Based on PDMS and PEG Side Chains for Fouling Release Applications. *Macromolecules* **2011**, *44*, 4783−4792.
(18) Sundaram, H. S.; Cho, Y.; Dimitriou, M. D.; Finlay, J. A.; Cone, G.; Williams, S.; Handlin, D.; Gatto, J.; Callow, M. E.; Callow, J. A.; Kramer, E. J.; Ober, C. K. Fluorinated Amphiphilic Polymers and Their Blends for Fouling-Release Applications: The Benefits of a Triblock Copolymer Surface. *ACS Appl. Mater. Interfaces* **2011**, *3*, 3366−3374.
(19) Weinman, C. J.; Finlay, J. A.; Park, D.; Paik, M. Y.; Krishnan, S.; Sundaram, H. S.; Dimitriou, M.; Sohn, K. E.; Callow, M. E.; Callow, J. A. ABC Triblock Surface Active Block Copolymer with Grafted Ethoxylated Fluoroalkyl Amphiphilic Side Chains for Marine Antifouling/Fouling-Release Applications. *Langmuir* **2009**, *25*, 12266−12274.
(20) Park, D.; Weinman, C. J.; Finlay, J. A.; Fletcher, B. R.; Paik, M. Y.; Sundaram, H. S.; Dimitriou, M. D.; Sohn, K. E.; Callow, M. E.; Callow, J. A.; Handlin, D. L.; Willis, C. L.; Fischer, D. A.; Kramer, E. J.; Ober, C. K. Amphiphilic Surface Active Triblock Copolymers with Mixed Hydrophobic and Hydrophilic Side Chains for Tuned Marine Fouling-Release Properties. *Langmuir* **2010**, *26*, 9772−9781.
(21) Dimitriou, M. D.; Zhou, Z.; Yoo, H.-S.; Killops, K. L.; Finlay, J. A.; Cone, G.; Sundaram, H. S.; Lynd, N. A.; Barteau, K. P.; Campos, L. M. A General Approach to Controlling the Surface Composition of Poly (ethylene oxide)-Based Block Copolymers for Antifouling Coatings. *Langmuir* **2011**, *27*, 13762−13772.
(22) Lejars, M.; Margaillan, A.; Bressy, C. Fouling Release Coatings: A Nontoxic Alternative to Biocidal Antifouling Coatings. *Chem. Rev.* **2012**, *112*, 4347−4390.
(23) Zhu, X.; Loo, H.-E.; Bai, R. A Novel Membrane Showing both Hydrophilic and Oleophobic Surface Properties and Its Non-Fouling Performances for Potential Water Treatment Applications. *J. Membr. Sci.* **2013**, *436*, 47−56.
(24) Chen, W.; Su, Y.; Peng, J.; Dong, Y.; Zhao, X.; Jiang, Z. Engineering a Robust, Versatile Amphiphilic Membrane Surface through Forced Surface Segregation for Ultralow Flux-Decline. *Adv. Funct. Mater.* **2011**, *21*, 191−198.
(25) Chen, W.; Su, Y.; Peng, J.; Zhao, X.; Jiang, Z.; Dong, Y.; Zhang, Y.; Liang, Y.; Liu, J. Efficient Wastewater Treatment by Membranes through Constructing Tunable Antifouling Membrane Surfaces. *Environ. Sci. Technol.* **2011**, *45*, 6545−6552.
(26) Zhao, X.; Su, Y.; Li, Y.; Zhang, R.; Zhao, J.; Jiang, Z. Engineering Amphiphilic Membrane Surfaces Based on PEO and PDMS Segments for Improved Antifouling Performances. *J. Membr. Sci.* **2014**, *450*, 111−123.
(27) Lee, H.; Dellatore, S. M.; Miller, W. M.; Messersmith, P. B. Mussel-Inspired Surface Chemistry for Multifunctional Coatings. *Science* **2007**, *318*, 426−430.
(28) Kang, S. M.; Hwang, N. S.; Yeom, J.; Park, S. Y.; Messersmith, P. B.; Choi, I. S.; Langer, R.; Anderson, D. G.; Lee, H. One-Step Multipurpose Surface Functionalization by Adhesive Catecholamine. *Adv. Funct. Mater.* **2012**, *22*, 2949−2955.
(29) Cao, Y.; Zhang, X.; Tao, L.; Li, K.; Xue, Z.; Feng, L.; Wei, Y. Mussel-Inspired Chemistry and Michael Addition Reaction for Efficient Oil/Water Separation. *ACS Appl. Mater. Interfaces* **2013**, *5*, 4438−4442.
(30) Ye, Q.; Zhou, F.; Liu, W. Bioinspired Catecholic Chemistry for Surface Modification. *Chem. Soc. Rev.* **2011**, *40*, 4244−4258.
(31) Waite, J. H. Surface Chemistry: Mussel Power. *Nat. Mater.* **2008**, *7*, 8−9.
(32) LaVoie, M. J.; Ostaszewski, B. L.; Weihofen, A.; Schlossmacher, M. G.; Selkoe, D. J. Dopamine Covalently Modifies and Functionally Inactivates Parkin. *Nat. Med.* **2005**, *11*, 1214−1221.
(33) Lee, H.; Rho, J.; Messersmith, P. B. Facile Conjugation of Biomolecules onto Surfaces via Mussel Adhesive Protein Inspired Coatings. *Adv. Mater.* **2009**, *21*, 431−434.
(34) Kasemset, S.; Lee, A.; Miller, D. J.; Freeman, B. D.; Sharma, M. M. Effect of Polydopamine Deposition Conditions on Fouling Resistance, Physical Properties, and Permeation Properties of Reverse Osmosis Membranes in Oil/Water Separation. *J. Membr. Sci.* **2013**, *425−426*, 208−216.
(35) Sabde, A. D.; Trivedi, M. K.; Ramachandhran, V.; Hanra, M. S.; Misra, B. M. Casting and Characterization of Cellulose Acetate Butyrate Based UF Membranes. *Desalination* **1997**, *114*, 223−232.
(36) Bernsmann, F.; Ball, V.; Addiego, F. D. R.; Ponche, A.; Michel, M.; Gracio, J. J. D. A.; Toniazzo, V. R.; Ruch, D. Dopamine-Melanin Film Deposition Depends on the Used Oxidant and Buffer Solution. *Langmuir* **2011**, *27*, 2819−2825.
(37) Jiang, J.; Zhu, L.; Zhu, L.; Zhu, B.; Xu, Y. Surface Characteristics of a Self-Polymerized Dopamine Coating Deposited on Hydrophobic Polymer Films. *Langmuir* **2011**, *27*, 14180−14187.
(38) Wei, Q.; Zhang, F.; Li, J.; Li, B.; Zhao, C. Oxidant-Induced Dopamine Polymerization for Multifunctional Coatings. *Polym. Chem.* **2010**, *1*, 1430−1433.
(39) Zangmeister, R. A.; Morris, T. A.; Tarlov, M. J. Characterization of Polydopamine Thin Films Deposited at Short Times by Autoxidation of Dopamine. *Langmuir* **2013**, *29*, 8619−8628.
(40) Owens, D. K.; Wendt, R. Estimation of the Surface Free Energy of Polymers. *J. Appl. Polym. Sci.* **1969**, *13*, 1741−1747.
(41) Magin, C. M.; Cooper, S. P.; Brennan, A. B. Non-Toxic Antifouling Strategies. *Mater. Today* **2010**, *13*, 36−44.
(42) Krishnan, S.; Weinman, C. J.; Ober, C. K. Advances in Polymers for Anti-Biofouling Surfaces. *J. Mater. Chem.* **2008**, *18*, 3405−3413.
(43) Zhao, X.; Su, Y.; Chen, W.; Peng, J.; Jiang, Z. Grafting Perfluoroalkyl Groups onto Polyacrylonitrile Membrane Surface for Improved Fouling Release Property. *J. Membr. Sci.* **2012**, *415−416*, 824−834.
(44) Lee, H.; Scherer, N. F.; Messersmith, P. B. Single-Molecule Mechanics of Mussel Adhesion. *Proc. Natl. Acad. Sci. U. S. A.* **2006**, *103*, 12999−13003.
(45) Wei, X.; Kong, X.; Sun, C.; Cheng, J. Characterization and Application of a Thin-Film Composite Nanofiltration Hollow Fiber Membrane for Dye Desalination and Concentration. *Chem. Eng. J.* **2013**, *223*, 172−182.
(46) Liu, M.; Zheng, Y.; Shuai, S.; Zhou, Q.; Yu, S.; Gao, C. Thin-Film Composite Membrane Formed by Interfacial Polymerization of Polyvinylamine (PVAm) and Trimesoyl Chloride (TMC) for Nanofiltration. *Desalination* **2012**, *288*, 98−107.
(47) Zheng, Y.; Yu, S.; Shuai, S.; Zhou, Q.; Cheng, Q.; Liu, M.; Gao, C. Color Removal and COD Reduction of Biologically Treated Textile Effluent through Submerged Filtration Using Hollow Fiber Nanofiltration Membrane. *Desalination* **2013**, *314*, 89−95.

(48) Hu, M.; Mi, B. Enabling Graphene Oxide Nanosheets as Water Separation Membranes. *Environ. Sci. Technol.* **2013**, *47*, 3715−3723.
(49) Misra, A.; Jarrett, W. L.; Urban, M. W. New Poly (methyl methacrylate)/N-butyl acrylate/Pentafluorostyrene/Poly (ethylene glycol)(p-MMA/nBA/PFS/PEG) Colloidal Dispersions: Synthesis, Film Formation, and Protein Adsorption. *Macromolecules* **2009**, *42*, 7299−7308.
(50) Shukla, R.; Cheryan, M. Performance of Ultrafiltration Membranes in Ethanol−Water Solutions: Effect of Membrane Conditioning. *J. Membr. Sci.* **2002**, *198*, 75−85.
(51) Peng, J.; Su, Y.; Chen, W.; Zhao, X.; Jiang, Z.; Dong, Y.; Zhang, Y.; Liu, J.; Cao, X. Polyamide Nanofiltration Membrane with High Separation Performance Prepared by EDC/NHS Mediated Interfacial Polymerization. *J. Membr. Sci.* **2013**, *427*, 92−100.
(52) Liu, Q.; Wang, N.; Caro, J.; Huang, A. Bio-Inspired Polydopamine: A Versatile and Powerful Platform for Covalent Synthesis of Molecular Sieve Membranes. *J. Am. Chem. Soc.* **2013**, *135*, 17679−17682.